Table I. Results of Comparisons of Relaxation Theory for Hyperfine-Coupled[a] Cu^{2+} Ions with the 25 °C NMRD Profiles of Various Cu^{2+}-Protein Complexes, at Different Solvent Viscosities Adjusted by Sucrose

protein	η/η_0	r_{Cu-H},[a] Å	τ_c,[b] ns	θ,[c] deg
Cu_2TRN[d]	1.0	3.6	6.4	42
Cu_2TRN[d]	2.2	3.6	6.0	53
Cu_2Zn_2SOD[e,f]	1.0	3.4	2.4	15
Cu_2Zn_2SOD[e]	5.9	3.4	2.9	26

[a] Calculated assuming a single water molecule, in rapid exchange, interacting with each Cu^{2+} with its protons equidistant from the ion. [b] It is assumed, as in other Cu^{2+}-protein systems, that τ_s can be equated to the derived correlation time. The estimated uncertainty on τ_c is ±10%. [c] θ is the angle between the direction of r_{Cu-H} and the unique axis of the hyperfine tensor for the interaction of a Cu^{2+} ion with its nucleus. This parameter is required by the theoretical treatment, but the results are relatively insensitive to its value. [d] Samples in 44 mM HCO_3^{-1} buffer at pH 8.3. Fitting done using $A_\parallel = 168 \times 10^{-4}$ cm^{-1} and $A_\perp = 20 \times 10^{-4}$ cm^{-1}. [e] Samples, unbuffered, at pH 5.1. Fitting done using $A_\parallel = 143 \times 10^{-4}$ cm^{-1} and $A_\perp = 20 \times 10^{-4}$ cm^{-1}. [f] The data for the superoxide dismutase for $\eta/\eta_0 = 1$ yield a somewhat longer τ_c and larger r_{Cu-H} than do earlier data[13] taken near neutral pH and also required a smaller $A_\perp$ value for a satisfactory fit. This could indicate that at lower pH the ligand field of the copper chromophore becomes somewhat more axial; the conclusions drawn in the present paper, however, remain unaffected.

Even if there are no explicit estimates, a variation of more than a factor of 2 in linewidth would provide linewidths either at the limit of detection or extraordinarily sharp, which is rare. As suggested by a reviewer, we also measured the EPR spectra of SOD in the presence and absence of sucrose. The EPR data, shown in Figure 4, are consistent with T_{2e} values of 1.8×10^{-9} or 2.1×10^{-9} s for the $\eta/\eta_0 = 1$ and the $\eta/\eta_0 = 5.9$ samples, respectively; these values compare exceedingly well with the T_{1e} values reported in Table I. It should be pointed out, however, that T_{2e}^{-1} is not expected to decrease with increasing τ_r as T_{1e}^{-1} does outside the so-called fast motion regime, even in the presence of rotational mechanisms. Therefore T_{2e} data cannot be easily used to prove or disprove any particular mechanism.

The present NMRD experiments demonstrate that τ_r has no influence on the electronic relaxation processes. Therefore, the modulation of the interaction energy between the electron and the lattice[24] has to occur through nonrotational mechanisms, such as vibration distribution of phonon type in a "microcrystal" formed by the metal and the protein as suggested by Kivelson,[25] although he concluded from his data that vibrational mechanisms might not be the major source of relaxation in solution. For small complexes ($\tau_r < 10^{-10}$ s) rotational mechanisms related to eq 5 have been shown to account for the observed T_{1e}^{-1}. However, the similar splitting of the d orbitals in small and large molecules of similar geometry (which determine g and A anisotropy) and the similar EPR linewidth may suggest that also in small complexes the nonrotational mechanism here proposed can concur to determine electron relaxation.

(24) Orbach, R. *Proc. Phys. Soc., London* **1961**, *A77*, 821.
(25) Kivelson, D. *J. Chem. Phys.* **1966**, *45*, 1324.

Structural Models for Non-Oxide Chalcogenide Glasses. Atomic Distribution and Local Order in the System Phosphorus–Selenium Studied by ^{31}P Dipolar NMR Spectroscopy

David Lathrop and Hellmut Eckert*

Contribution from the Department of Chemistry, University of California at Santa Barbara, Goleta, California 93106. *Received October 31, 1988*

Abstract: Homonuclear dipolar coupling information encoded in solid-state NMR spectra affords a quantitative criterion for the test of structural hypotheses for non-oxide chalcogenide glasses. Using a selective spin-echo sequence, ^{31}P–^{31}P dipolar second moments have been measured for glasses in the system phosphorus–selenium (10–50 atom % P) and related model compounds. The results are in striking contrast to the preliminary structural hypotheses raised with the aid of competing spectroscopic techniques. The NMR results can be simulated quantitatively in terms of a random distribution of P and Se atoms over a cubic lattice with a decidedly preferential formation of P–Se over P–P bonds. Up to 25 atom % P, the phosphorus atoms are entirely coordinated to selenium, whereas in glasses with higher P contents, P–P bonds are introduced in less than purely statistical proportions. The NMR results show no indication of units with intermediate-range order, such as the P_4Se_n clusters inferred from neutron diffraction and EXAFS work.

1. Introduction

Non-oxide chalcogenide glasses, which are based on the sulfides, selenides, and tellurides of the main group III–V elements, have recently gained much interest for semiconductors, photoconductors, solid electrolytes, and low-frequency waveguide materials.[1] Because of these technologically attractive properties, the structural arrangement in these systems has recently received considerable attention. In spite of considerable efforts, there is still no good microscopic structural model that provides a comprehensive description of the principles of glass formation, the atomic environments, and their distribution in these systems. The various models developed for different, but chemically related, systems diverge dramatically in their fundamental concepts. As an example, the chaos implied in the "model of broken chemical order" postulated for As–Se and Ge–Se glasses[2,3] is in sharp contrast to

(1) Taylor, P. C. *Mater. Res. Soc. Bull.* **1987**, 36.
(2) Phillips, J. C. *J. Noncryst. Solids* **1981**, *43*, 37.
(3) Boolchand, P. *Hyperfine Interact.* **1986**, *27*, 3.

0002-7863/89/1511-3536$01.50/0

the postulate of intermediate range in addition to short-range order inferred to exist in silicon chalcogenide glasses.[4] Sometimes, even the structural models that have been suggested for a given system have remained controversial, partly because many models rely on methods that are either difficult to relate to structural properties (T_g, viscosity measurements), are not inherently quantitative (EXAFS, Raman), or tend to emphasize the contribution of ordered environments (diffraction methods).

Regarding the latter statement, the glass system phosphorus–selenium provides an interesting example. The phase diagram and the region of glass formation have been published ca. 15 years ago, and the bulk thermodynamical properties of these glasses are well characterized.[5-11] Homogeneous glasses can be formed at compositions ranging from 0 to 52 mol % phosphorus; a second, smaller region of glass formation is found between 62 and 80 mol % P. The only well-characterized crystalline compound remains P_4Se_3,[12] although crystalline compounds with stoichiometries P_4Se_4 and P_4Se_5 have also been reported.[13,14] Selenium analogues of the sulfide compounds P_4S_7, P_4S_9, and P_4S_{10} are not known. Attempts at synthesizing such compounds have resulted in glasses extremely resistant toward recrystallization. Recently, these glasses have been studied extensively by modern spectroscopic techniques, such as EXAFS, Raman, and FTIR spectroscopy and neutron diffraction.[15-17] From these studies, an interesting controversy regarding the structural organization of these glasses has emerged. On the one hand, Borisova et al.[5-7] as well as Blachnik and co-workers[8] propose what basically amounts to a chemically ordered continuous random network model: at phosphorus contents below 40 mol %, the glasses contain Se=$PSe_{3/2}$, $PSe_{3/2}$, and Se–Se units only, whereas no P–P bonds exist. Above 40 mol %, P, these authors suggest an abrupt increase in the fraction of P–P bonds, hence rationalizing the steep increase of glass transition temperatures, which is experimentally observed in this compositional region.

In sharp contrast, the EXAFS and neutron diffraction studies point toward an entirely different glass structure based on P_4Se_n clusters ($5 \leq n \leq 3$, depending on the P/Se ratio), which are embedded in a Se-rich matrix.[15,16] Such an arrangement constitutes substantial intermediate range order, such as recently suggested for other glass systems.

In the present study, we have used a selective pulsed solid-state NMR technique to shed some light on this controversy. The usefulness of solid-state NMR in addressing structural questions in glasses stems from the presence of terms in the spin Hamiltonian which produce perturbations of the main interaction of the nuclear spins with the external magnetic field. These perturbations, which include chemical shielding and dipole–dipole couplings, are readily determined experimentally and can be connected with chemical information by modelling studies or by comparison with crystalline reference compounds. While, during the course of widespread application to oxidic glasses in the past two decades, NMR techniques have proven instrumental in developing new approaches toward glass structure concepts,[18] the present study represents one of the first systematic applications of modern NMR techniques to non-oxide chalcogenide glasses. Figure 1 shows three conceivable atomic distribution models for P–Se glasses, corresponding to (a) a uniform, (b) a clustered, and (c) a random distribution of P atoms. These arrangements should be distinguishable by the magnitude and the compositional dependence of the dipole–dipole couplings between the ^{31}P nuclear spins. Thus, in contrast to the large majority of modern NMR studies of glasses, which rely on chemical shift comparisons for structural assignments, this study is concerned with the experimental determination and the modelling of ^{31}P–^{31}P dipole–dipole couplings in glasses. We will examine the previously proposed structural models for P–Se glasses in the light of our measurements, propose an alternative model that is more compatible with our results, and discuss the general implications for the development of structural models for non-oxide chalcogenide glasses.

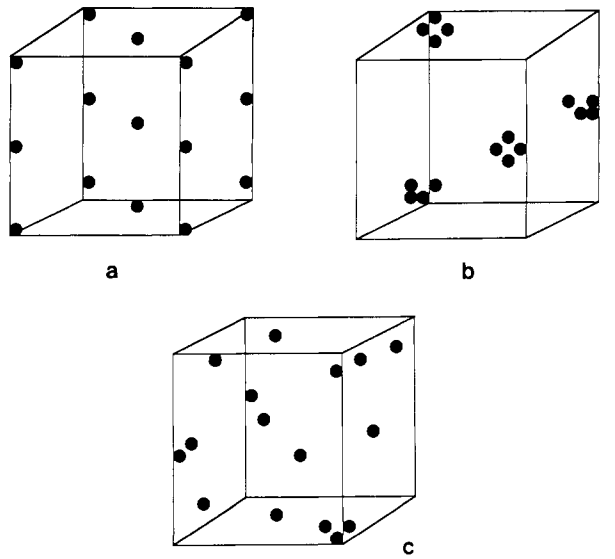

Figure 1. Proposed and conceivable models for the distribution of P atoms over the structure of P–Se glasses: (a) uniform distribution, (b) clustered distribution involving P_4Se_n entities as proposed in ref 15, (c) random distribution.

2. Fundamental Concepts and Methodology

A variety of modern pulsed NMR methods are available to measure homonuclear dipole–dipole couplings, including zero-field,[19] nutation,[20] and multiple-quantum NMR.[21,22] These methods are especially powerful in characterizing small, well-separated entities, whose dipolar couplings can be calculated from first principles. In contrast, the dipolar coupling in magnetically less dilute systems (such as the ones under study here), is usually expressed in terms of a statistical quantity, the second moment M_{2d} of the resonance line. Assuming the dominance of homonuclear dipole–dipole couplings over other types of anisotropic perturbations in the solid state, the second moment M_{2d} can be calculated from the internuclear distances d_{ij} by the van Vleck theory,[23] which in the case of a polycrystalline material predicts:

$$M_{2d} = {}^3/_5(\mu_0/4\pi)^2 I(I+1)\gamma^4\hbar^2 N^{-1}\sum d_{ij}^{-6} \quad (1a)$$

or

$$M_{2d} = {}^4/_{15}(\mu_0/4\pi)^2 I(I+1)\gamma^4\hbar^2 N^{-1}\sum d_{ij}^{-6} \quad (1b)$$

where γ is the gyromagnetic ratio of the nucleus under consid-

(4) Tenhover, M.; Hazle, M. A.; Grasselli, R. K. *Phys. Rev. Lett.* **1983**, *51*, 404.
(5) Borisova, Z. U. In *Glassy Semiconductors*; Plenum Press: New York, 1981; p 70.
(6) Borisova, Z. U.; Kasatkin, B. E.; Kim, E. I. *Izv. Akad. Nauk SSSR, Neorg. Mater.* **1973**, *9*, 822.
(7) Kim, E. I.; Chernov, A. P.; Dembovskii, S. A.; Borisova, Z. U. *Izv. Akad Nauk SSSR, Neorg. Mater.* **1976**, *12*, 1021.
(8) Blachnik, R.; Hoppe, A. *J. Noncryst. Solids* **1979**, *34*, 191.
(9) Monteil, Y.; Vincent, H. *J. Inorg. Nucl. Chem.* **1975**, *37*, 2053; *Z. Anorg. Allg. Chem.* **1977**, *428*, 259.
(10) Monteil, Y.; Vincent, H. *Can. J. Chem.* **1974**, *52*, 2190.
(11) Heyder, F.; D. Linke, D. *Z. Chem.* **1973**, *13*, 480.
(12) Keulen, E.; Vos, A. *Acta Crystallogr.* **1959**, *12*, 323.
(13) Monteil, Y.; Vincent, H. *Z. Anorg. Allg. Chem.* **1975**, *416*, 181; Blachnik, R.; Hoppe, A. *Z. Anorg. Allg. Chem.* **1979**, *457*, 91.
(14) Penney, G. T.; Sheldrick, G. M. *J. Chem. Soc. A* **1971**, 245.
(15) Price, D. L.; Misawa, M.; Susman, S.; Morrison, T. I.; Shenoy, G. K.; Grimsditch, M. *J. Noncryst. Solids* **1984**, *66*, 443.
(16) Arai, M.; Johnson, R. W.; Price, D. L.; Susman, S.; Gay, M.; Enderby, J. E. *J. Noncryst. Solids* **1986**, *83*, 80.
(17) Kumar, A.; Malhotra, L. K.; Chopra, K. L. *J. Noncryst. Solids* **1987**, *92*, 51.
(18) Turner, G. L.; Kirkpatrick, R. J.; Risbud, S. H.; Oldfield, E. *Am. Ceram. Soc. Bull.* **1987**, *66*, 656. Muller-Warmuth, W.; Eckert, H. *Phys. Rep.* **1982**, *88*, 91.
(19) Weitekamp, D. P.; Bielecki, A.; Zax, D.; Zilm, K.; Pines, A. *Phys. Rev. Lett.* **1983**, *50*, 1807.
(20) Yannoni, C. S.; Kendrick, R. D. *J. Chem. Phys.* **1981**, *74*, 747.
(21) Baum, J.; Pines, A. *J. Am. Chem. Soc.* **1986**, *108*, 7447.
(22) Gleason, K. K.; Petrich, M. A.; Reimer, J. A. *Phys. Rev. B* **1987**, *36*, 3259.
(23) Van Vleck, J. H. *Phys. Rev.* **1948**, *74*, 1168.

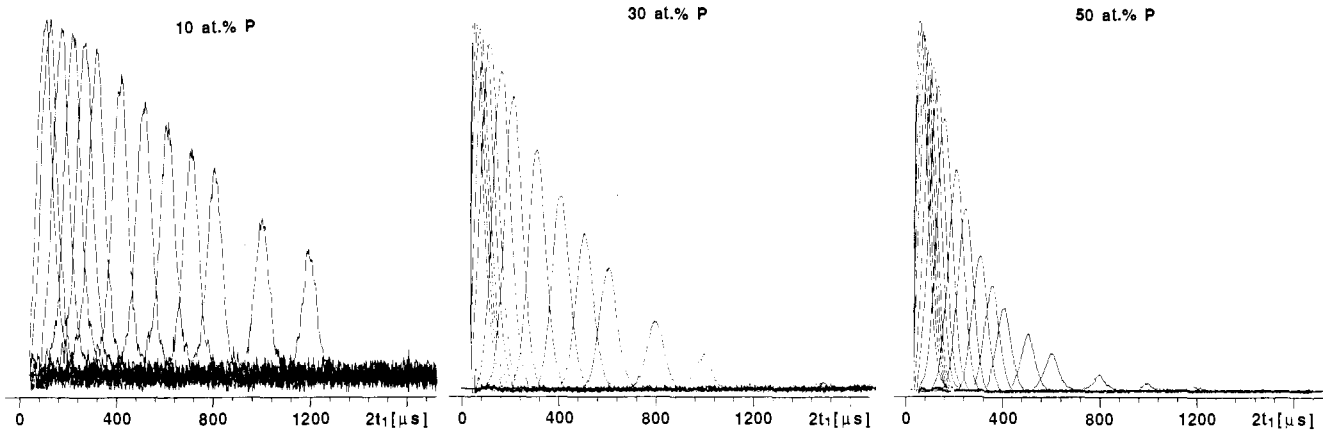

Figure 2. Dependence of the ^{31}P spin-echo amplitude on the evolution time $2t_1$ in three different P–Se glasses.

eration, I is the spin quantum number, and N is the number of nuclei involved. Equation 1a is appropriate, if the line shape is dominated by homogeneous broadening (due to homonuclear dipole–dipole coupling). Equation 1b has to be used, however, if inhomogeneous sources of line broadening (chemical shift anisotropy or chemical shift distribution) predominate, since the resulting spectral dispersion suppresses the quantum-mechanical ("flip–flop") term in the truncated dipolar Hamiltonian.[24]

Previous attempts to determine dipolar coupling strengths in P–Se glasses, using the traditional approach of field-dependent line-shape analyses,[25] have remained unsuccessful,[26-29] presumably because of the large error incurred upon the extrapolation to zero field strength. Alternatively, selective spin–echo techniques can be used to measure homonuclear spin–spin couplings.[30-38] In particular, the pulse sequence $90°-t_1-180°$ refocuses all interactions linear in I_z (i.e., heterodipolar $^{31}P-^{77}Se$ couplings, chemical shift anisotropies, and chemical shift distribution), resulting in formation of an echo at time $2t_1$. The height of this echo decreases with increasing t_1, because homonuclear $^{31}P-^{31}P$ spin–spin interactions are not refocussed. In the case of multiple spin interactions, the decay of the echo height $I(2t_1)$ as a function of $2t_1$ can often be approximated as a Gaussian:

$$I(2t_1)/I(0) = \exp\{-M_{2d}\,(2t_1)^2/2\}$$

Thus, the homonuclear dipolar second moment M_{2d} can be determined by spin–echo experiments with systematic incrementation of the evolution time $2t_1$. To obtain well-defined spin echoes, it is crucial that the strength of the interactions linear in I_z be at least comparable in magnitude to the $^{31}P-^{31}P$ dipolar coupling strength to be measured. An additional criterion, also satisfied in the present study, is that the couplings among the heteronuclei ($^{77}Se-^{77}Se$ in the present case) must be very weak relative to the P–Se coupling. These limitations may explain why problem-centered applications of this technique to materials have been scarce.[36-38] The present contribution will demonstrate the utility of spin–echo NMR for measuring the strength of homonuclear dipolar couplings in non-oxide chalcogenide glasses, hence providing a basis for a discussion of various bonding models in the P–Se glass system.

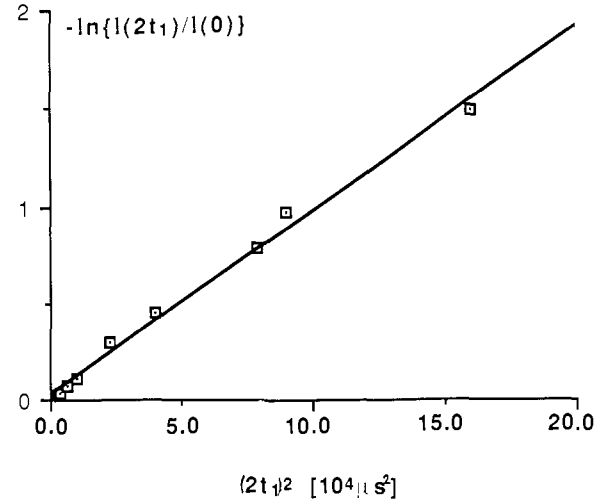

Figure 3. Plot of $-\ln\{I(2t_1)/I(0)\}$ vs evolution time $(2t_1)^2$ for a P–Se glass containing 40 atom % P.

3. Experimental Section

Sample Preparation and Characterization. Glasses containing 10–50 mol % phosphorus were prepared, according to literature methods, within evacuated Vycor ampoules, heated at 650 °C for 2 days, and quenched by turning off the furnace. All sample manipulations were carried out in a drybox. Glass transition temperatures were measured on a Dupont 912 dual sample differential scanning calorimeter, using heating rates of 5–10 °C/min. All glasses exhibit single glass-transition temperatures (T_g) in good agreement with literature values,[5-8] and none of them show any recrystallization behavior. Formation of completely amorphous samples was also verified by X-ray powder diffraction, using a Scintag diffractometer. Crystalline α-P_4Se_3 was obtained by slow cooling of a melt containing the elements in a stoichiometric ratio and subsequent recrystallization of the product from dried carbon disulfide. Identity and purity of the compound were verified by differential scanning calorimetry (mp 247 °C (lit. 246 °C), X-ray powder diffraction, and liquid-state NMR (doublet at −106 ppm, quartet at +37 ppm versus 85% H_3PO_4), in good agreement with literature data.[39] Crystalline P_4Se_4 was synthesized from P_4Se_3 and Se within the temperature interval 260–290 °C.[13] Differential scanning calorimetry shows the α to β phase transition at 298 °C (lit. 300 °C) and a melting point of 330 °C (lit. 330 °C).[13] No liquid-state ^{31}P NMR spectrum could be obtained owing to the apparent low solubility of this compound in CS_2 or other solvents. An

(24) Abragam, A. *The Principles of Nuclear Magnetism*; Clarendon Press: Oxford 1964.
(25) Van der Hart, D. L.; Gutowsky, H. S. *J. Chem. Phys.* **1968**, *49*, 261.
(26) Baidakov, L. A.; Shcherbakov, V. A. *Izv. Akad. Nauk SSSR, Neorg. Mater.* **1969**, *5*, 1882.
(27) Baidakov, L. A.; Borisova, Z. U. In *Amorphous and Liquid Semiconductors* (Proc. 5th Int. Conf.), Stuke, J., Brenig, W., Eds.; Taylor and Francis: London, 1974; p 1035.
(28) Baidakov, L. A.; Katruzov, A. N.; El Labani, H. M. *Izv. Akad. Nauk SSSR, Neorg. Mater.* **1978**, *14*, 1818.
(29) Eckert, H.; Muller-Warmuth, W. *J. Noncryst. Solids* **1985**, *70*, 199.
(30) Engelsberg, M.; Norberg, R. E. *Phys. Rev.* **1972**, *B5*, 3395.
(31) Mortimer, M.; Moore, E. A.; Apperley, D. C.; Oates, G. *Chem. Phys. Lett.* **1987**, *138*, 209.
(32) Warren, W. W., Jr.; Norberg, R. E. *Phys. Rev.* **1967**, *154*, 227.
(33) Boden, N.; Gibb, M.; Levine, Y. K.; Mortimer, M. *J. Magn. Reson.* **1974**, *16*, 471.
(34) Fenzke, D.; Freude, D.; Muller, D.; Schmiedel, H. *Phys. Status Solidi* **1972**, *50b*, 209.
(35) Pruski, M.; Ernst, H.; Pfeifer, H.; Staudte, B. *Chem. Phys. Lett.* **1985**, *119*, 412.
(36) Douglass, D. C.; Duncan, T. M.; Walker, K. L.; Csencsits, R. *J. Appl. Phys.* **1985**, *58*, 197.
(37) Duncan, T. M.; Douglass, D. C.; Csencsits, R.; Walker, K. L. *J. Appl. Phys.* **1986**, *60*, 130.
(38) Reimer, J. A.; Duncan, T. M. *Phys. Rev. B* **1983**, *27*, 4895.
(39) Blachnik, R.; Wickel, U.; Schmitt, P. *Z. Naturforsch., Teil B* **1984**, *39*, 1135.

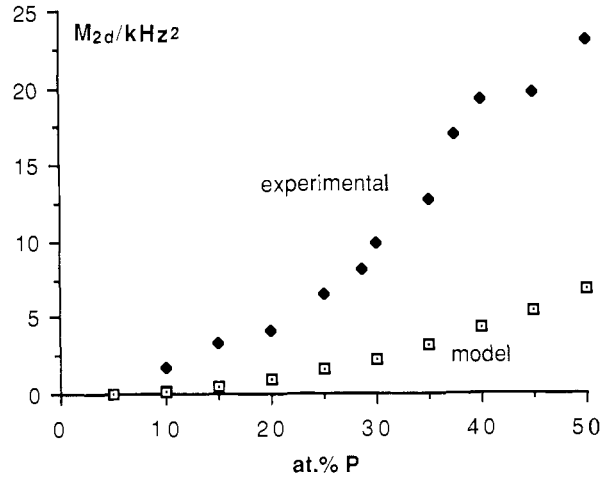

Figure 4. Compositional dependence of M_{2d} in P–Se glasses. Comparison of experimental data with the values calculated for a uniform distribution of P atoms.

attempt to reproduce the previously reported synthesis of P_4Se_5[14] was unsuccessful. The synthesis, characterization, and MAS-NMR properties of several crystalline phosphorus sulfides, used as additional reference materials, is reported elsewhere.[40]

Nuclear Magnetic Resonance Studies. All NMR studies were carried out at 121.65 MHz (field strength 7.05 T), using a General Electric GN-300 spectrometer system and a multinuclear probe from Doty Scientific. The 90° pulse length was 7.0–8.5 μs. To ensure quantitative signal detection, spin–lattice relaxation times were estimated by progressive saturation experiments. All spin–echo experiments were done under conditions of minimized resonance offsets and spin–equilibrium conditions; this necessitated recycle delays of up to 60 min.

4. Results and Interpretation

Figure 2 shows a typical collection of spin echos as a function of evolution time $2t_1$ for three glass compositions. To test for Gaussian character of this decay, ln $\{I(2t_1)/I(0)\}$ was plotted against $(2t_1)^2$. Figure 3 shows that the decay is Gaussian in character over a wide range of $2t_1$ ($2t_1 \leq 300$ μs). At larger evolution times, the decay amplitudes deviate from the Gaussian behavior of Figure 3. Linear regression fits have been obtained for all samples within the time interval $0 \leq 2t_1 \leq 300$ μs. Table I lists the M_{2d} values thus obtained.

Table II shows the corresponding experimental values for several crystalline phosphorus sulfides and selenides and the model compounds GaP and InP. The experimental data obtained for these compounds are compared with the values calculated from the van Vleck theory (see Table I), using the known lattice positions in the crystal structures of these model compounds[41–43] and including all P–P distances within 20 Å. In these calculations, eq 1a was used for InP and GaP, since the chemical shift anisotropy and dispersion vanish in these cubic compounds, whereas eq 1b was used for the crystalline phosphorus sulfides and selenides, in which the chemical shift anisotropy is large. In particular, our experimental results on InP are in good agreement with those obtained by Engelsberg and Norberg.[30] The experimental value for GaP is lower than calculated, presumably because the required condition M_2(Ga–P) $\gg$ M_2(P–P) is not satisfied in this compound.[31] The opposite deviation observed for P_4S_{10} may arise from the fact that a situation intermediate to eq 1a and 1b applies for the dipolar coupling (the four P atoms are almost equivalent, and a multitude of crystallite orientations exists, at which at least two P atoms are essentially isochromatic). The latter complication is unlikely to occur in our measurements of the glasses since ^{31}P MAS-NMR data indicate that a very wide chemical shift distribution exists in these glasses.[44]

(40) Eckert, H.; Liang, C. S.; Stucky, G. D. *J. Phys. Chem.* **1989**, *93*, 452.
(41) Vos, A.; Wiebenga, E. H. *Acta Crystallogr.* **1955**, *8*, 217.
(42) Vos, A.; Olthof, R.; Van Bolhuis, F.; Botterweg, R. *Acta Crystallogr.* **1965**, *19*, 864.
(43) Minshall, P. C.; Sheldrick, G. M. *Acta Crystallogr.* **1978**, *B34*, 1326.
(44) Lathrop, D.; Eckert, H., *J. Noncryst. Solids* **1988**, *106*, 417.

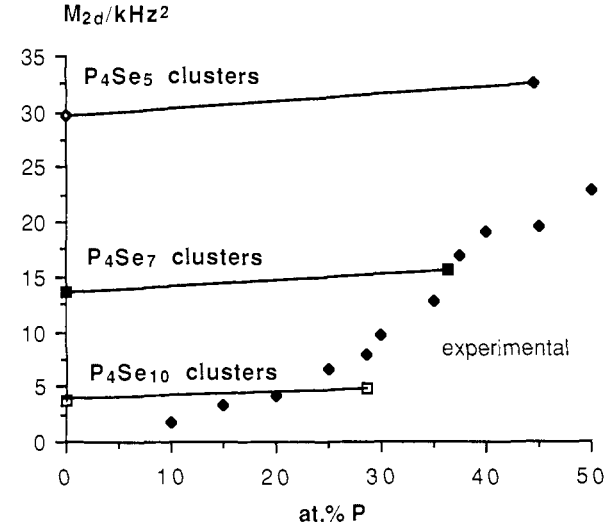

Figure 5. Compositional dependence of M_{2d} in P–Se glasses. Comparison of experimental data with the values calculated for various cluster models as proposed in the literature.

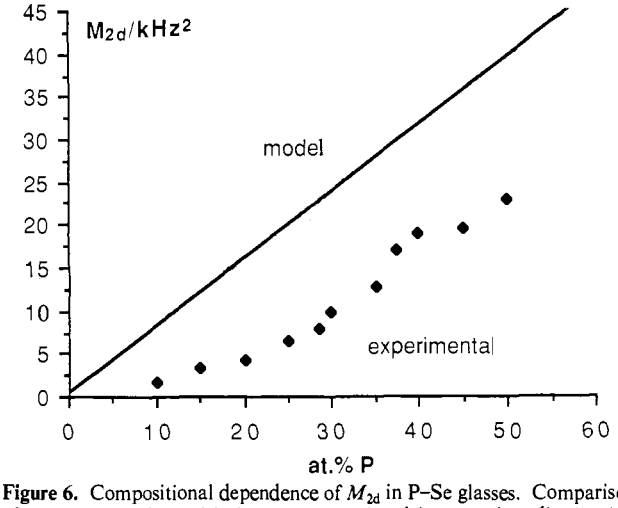

Figure 6. Compositional dependence of M_{2d} in P–Se glasses. Comparison of experimental data with the values calculated for a random distribution of P and Se atoms over a zinc blende lattice (see text).

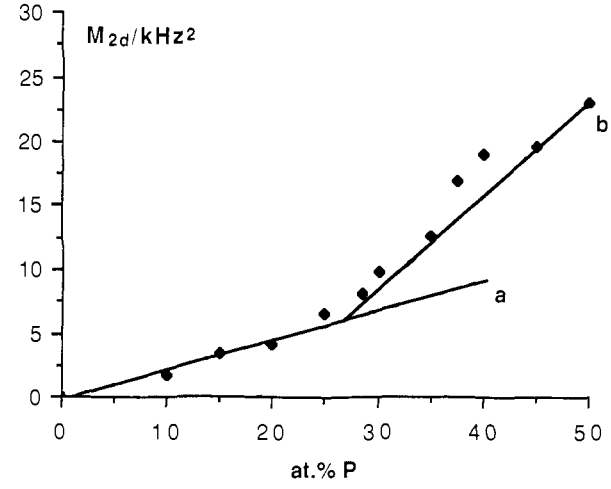

Figure 7. Compositional dependence of M_{2d} in P–Se glasses. Comparison of experimental data with the values calculated for a tailored random distribution of P and Se atoms over a zinc blende lattice (a) excluding P–P bonds entirely, and (b) allowing P–P bonds to occur with the reduced probability of $(X - 25)$% for glasses containing X% phosphorus.

The compositional dependence of M_{2d} in P–Se glasses is shown in Figures 4–7 indicating a monotonic increase of ^{31}P–^{31}P homonuclear interactions with increasing phosphorus content. The

Table I. M_{2d} Values Obtained for P–Se Glasses

atom % P	M_{2d} (kHz^2) (±10%)	atom % P	M_{2d} (kHz^2) (±10%)
10	1.9	35	12.6
15	3.4	37.5	17.0
20	4.1	40	19.0
25	6.5	45	19.6
28.6	7.3	50	23.0
30	9.8		

Table II. Experimental and Calculated M_{2d} Values (±10%) for Crystalline Reference Compounds and Assumed Clusters

compound	M_{2d} (kH$_2^2$) exp	M_{2d} (kH$_2^2$) calcd
P_4Se_4 (cluster)[a]		22.6
P_4Se_5 (crystal)		30.6
P_4Se_5 (cluster)		27.4
P_4Se_5 (crystal)[a]		32.6
P_4Se_5 (cluster)[a]		29.7
P_4Se_7 (crystal)[a]		15.6
P_4Se_7 (cluster)[a]		13.6
P_4Se_{10} (crystal)[a]		4.8
P_4Se_{10} (cluster)[a]		3.8
P_4Se_3	44.6	41.8
P_4Se_4[a]	22.2	26.1
P_4S_7	19.0	18.5
P_4S_{10}	9.9	7.1
GaP	20.7	30.3
InP	21.0	19.5
P(red)[b]	61.0	57.2

[a] Calculated values assume hypothetical structures by scaling the dimensions, excluding P–P bond lengths, from the known lattice geometries of the stoichiometry-analogue sulfide compounds. [b] Calculated value assumes a uniform distribution of P atoms.

data are compared with theoretically calculated second moments (including P–P distances up to 10–20 Å) assuming four models discussed below: (a) a uniform distribution of P atoms, based on an avoidance of P–P proximities, Figure 4; (b) models invoking various P_4Se_n microclusters in a Se-rich matrix, as suggested by EXAFS and neutron diffraction data, Figure 5; (c) a random distribution of P and Se atoms over the lattice positions of a zinc blende structure, Figure 6; (d) a tailored random distribution of P and Se atoms over the lattice positions of a zinc blende structure, assuming a preference of P–Se bonds over P–P bonds, Figure 7. The inherent assumptions of these various models are described below.

A. Uniform Distribution Model. The uniform distribution model was simulated by arranging the number of P atoms per cm^3 (calculated from the P and Se contents and the experimental densities[5]) in a cubic lattice. This model corresponds to maximized P–P distances.

B. Cluster Models. Three cluster models involving P_4Se_{10}, P_4Se_7, and P_4Se_5 clusters interconnected by Se_n chains were simulated. To calculate M_{2d} values for the limit of isolated clusters (in glasses with P contents approaching zero), we assumed hypothetical molecules with geometries identical with those known in the analogous P–S systems.[41-43] However, to account for the longer P–Se (compared to P–S) bond length, all dimensions, excluding P–P bonds, were increased by ca. 7%. The dipolar coupling within the clusters was then modelled in terms of the intramolecular ^{31}P–^{31}P second moments calculated for these hypothetical molecules. Using a similar scaling approach, M_{2d} values for the limit of the glass compositions corresponding to the respective cluster stoichiometries were calculated from the known crystal structures of the analogue phosphorus sulfides including all P atoms within 20-Å distance. This scaling procedure is validated by the good agreement (see Table II) between the M_{2d} value thus calculated for P_4Se_5 and the value obtained by using the atomic coordinates for the actual structure from the study by Penney and Sheldrick.[14] For modelling glass compositions between the above limits, M_{2d} was linearly interpolated between the cluster value and the full structural value.

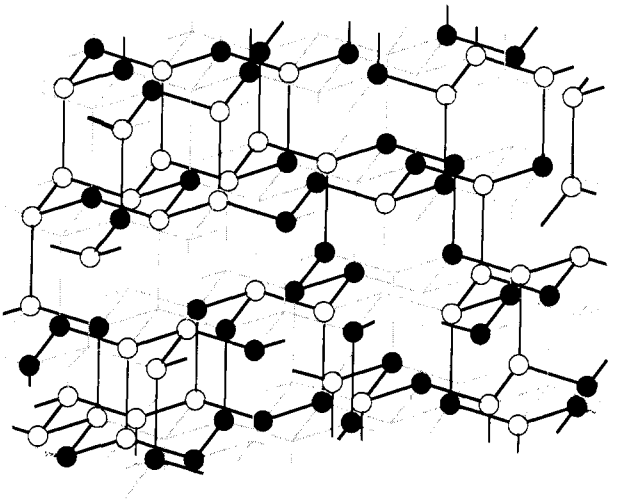

Figure 8. Graphical illustration of the randomly occupied zinc blende structure used as a model for a P–Se glass containing 50 atom % P. Open circles denote P atoms, filled circles Se atoms. The dotted lines represent nonbonding electron pairs pointing toward a vacancy in the structure.

C. Random Distribution Model. Since P–P, P–Se, and Se–Se bond lengths are almost identical, a chemically reasonable model of local bonding in these glasses can be obtained by distributing P and Se atoms irregularly over the atomic positions of a covalent lattice. For our present glass system, we chose the zinc blende structure, since it is one of the preferred lattice types for many chemically related sulfides and selenides. P and Se atoms were distributed randomly according to their atomic percentages. A lattice constant of 5.289 Å was chosen, corresponding to nearest-neighbor distances of 2.29 Å (average of typical P–P, P–Se, and Se–Se bond lengths). Furthermore, the valency constraints of P and Se were incorporated by distributing nonbonding electron pairs over additional lattice positions. One such lattice position was assumed to accept four lone pairs. The resulting model reproduces the experimental densities of all the glasses within 5–10%. The dipolar second moment at each concentration was then calculated for 200 different P atoms over a range of 10 Å, and averaged. Figure 8 shows a graphical illustration of this model.

For simplicity, it is assumed that all of the P atoms are three-coordinate (one lone pair), and all of the Se-atoms two-coordinate (two lone pairs); however, incorporation of some four-coordinate P atoms and one-coordinate Se atoms into this model is unlikely to change results and conclusions significantly.

D. Tailored Random Distribution Model. The above model was modified to exclude P atoms in the first coordination sphere around P for glasses up to 40 atom % P. This model leads to close agreement with the experimental M_{2d} values for glasses below ca. 25 atom % P (curve a in Figure 7). Therefore, the region from 25 to 50 atom % P was modelled by assuming that the probability of a P atom to appear in a particular site within the first coordination shell of phosphorus is 0% at 25 atm % P and $(X-25)$% at a glass composition of X atom % P. As shown in Figure 7, curve b, this calculation agrees very well with the experimental data in this composition range.

5. Discussion and Conclusions

We conclude from Figures 4–7 that the distribution of P atoms in the glass structure has to be viewed as random, rather than ordered. There is no tendency for the P atoms to maximize their respective distances, nor are our results compatible with proposed or conceivable cluster models. In particular, the existence of appreciable numbers of P_4Se_7 and P_4Se_5 clusters can be ruled out for all glasses with P contents below the compositions corresponding to the stoichiometries of these clusters. Likewise, the M_{2d} values measured for glasses with compositions near P_4Se_7, P_4Se_5, and P_4Se_4 stoichiometries are generally in the vicinity or somewhat lower than the values calculated from the hypothetical crystal structures scaled from their respective phosphorus sulfide

analogues. This result is in striking contrast to ref 15, which concludes that, at a given P/Se ratio, the amount of P–P bonding is significantly enhanced in the glasses, compared to the crystalline state.

The comparison of Figure 6 with Figure 7 indicates that, at any composition within the glass-forming region, there is a distinct preference for P–Se over P–P bonds. At low P contents ($0 \leq$ atom % P ≤ 25) the experimental M_{2d} values agree very well with a random distribution model that excludes P–P bonds entirely. However, the departure of the experimental data from the calculated line near 25 atom % P indicates that, in contrast to the contentions of ref 5–8, P–P bonds do contribute to the glass structure in this compositional region. They are, however, under-represented with respect to their statistical probability. For a glass containing 50 atom % P, and assuming one P nearest neighbor for each P atom, the tailored random distribution model yields an M_{2d} value of 27.6 kHz^2. The proximity to the experimental value of 23.0 kHz^2 indicates that the average number of P atoms adjacent to any particular P atom is in the vicinity of 1.0 (instead of 1.5, which is predicted from statistical probability) at this composition.

To check the model dependence of our conclusions, we examined the structural proposal, given in ref 8, for a glass containing 40 atom % P. Blachnik and Hoppe hypothesize that this glass consists of sheets based on $PSe_{3/2}$ units (no P–P bonds).[8] Assuming the atomic distribution as found in crystalline As_2Se_3[45] (with P atoms at the exact locations of the As sites), we calculate a ^{31}P dipolar second moment of 8.4 kHz^2, which is significantly below the experimental value.[46] Thus, our conclusion that significant amounts of P–P bonds exist at and below 40 atom % P remains the same even when considering an entirely different structural model.

In summary, selective spin–echo NMR has proven a powerful method of measuring ^{31}P–^{31}P dipolar second moments in non-oxide chalcogenide glasses. These data provide a crucial test for the structural models postulated on the basis of competing techniques. The NMR results can be understood in terms of a random distribution of P and Se atoms over a glass structure modelled as a defect zinc blende lattice, excluding P–P bonds below 25 atom % P and admitting them in less than statistical proportions above 25%.

The modified defect zinc blende model discussed above should be understood as a simple framework enabling discussion of conceivable atomic distribution models in P–Se glasses, rather than as a structural hypothesis. The M_{2d} value will be fairly insensitive toward the introduction of further disorder, via bond length and angle dispersions, additional P=Se bonds, or valence alternation pairs.[47] By the same token, however, our conclusion regarding P–Se vs. P–P bonding in these glasses is fairly model-independent as well. There is no evidence for significant amounts of discrete P_4Se_n clusters, and the distribution of P atoms over the glass structure shows none of the features characteristic of the "intermediate range order" inferred from the application of other techniques. This conclusion may be significant for the development of more sophisticated quantitative structural models for non-oxide chalcogenide glasses in the future.

Acknowledgment. Financial support of this research by the UCSB Academic Senate is gratefully acknowledged.

Registry No. P, 7723-14-0; Se, 7782-49-2.

(45) Stergiou, A. C.; Rentzeperis, P. J. *Z. Kristallogr.* **1985**, *173*, 185.

(46) In this calculation, no bond length scaling was assumed, since the density of this assumed P_2Se_3 crystal structure (3.98 g/cm^3) was already significantly above the experimental value for the glass, 3.55 g/cm^3. If the As–Se bond lengths are scaled down from 2.42 to 2.25 Å, the density increases to the unrealistically high value of 4.5 g/cm^3. Even then, the calculated M_{2d} value of 13.2 kHz^2 is still significantly lower than the experimental value in the glass.

(47) Dembovskii, S. A.; Chechetkina, E. A. *J. Noncryst. Solids* **1986**, *85*, 364.